LMSS DRIVE SIMULATOR FOR MULTIPATH PROPAGATION

Praveen Vishakantaiah, Wolfhard J. Vogel

Electrical Engineering Research Laboratory
The University of Texas at Austin
10100 Burnet Rd., Austin, TX 78758

Abstract--A three-dimensional drive simulator for the prediction of LMSS multipath propagation has been developed. It is based on simple physical and geometrical rules and can be used to evaluate effects of scatterer numbers and positions, receiving antenna pattern, and satellite frequency and position. It is shown that scatterers close to the receiver have the most effect and that directive antennas suppress multipath interference.

1. Introduction

Land mobile satellite service (LMSS) is a new communications system which exploits the strengths of satellites: continental coverage and mobility. It will enable telephone and data service to vehicles traveling throughout the US, especially in rural areas, away from mayor traffic arteries, where terrestrial cellular service may never be established. The design of this system is currently under way and the selection of optimal system parameters, such as antenna pattern, modulation, and coding, requires the knowledge of propagation impairments.

At L band, the intended frequency of LMSS, the two major propagation effects are: (1) fading caused by obstructions in the line-of-sight path between the vehicle and the satellite, and (2) fading caused by the interference of the direct wave with reflections from scatterers all around the vehicle. Several approaches have been followed to quantify propagation effects. Initially, hard- [Davarian, 1987] and software [Divsalar, 1985] simulators were developed based on statistical assumptions of shadowed multipath propagation derived from terrestrial mobile propagation (Ricean and/or Rayleigh multipath, log-normal shadowing). Subsequently, many field measurements of propagation effects were made [see References in Vogel, Goldhirsh, and Hase, 1989], and their results were used to develop empirical [Vogel, Goldhirsh, and Hase, 1989] and semi-empirical [Barts et al, 1987] propagation models. Recently, measurement results have also been used for refining simulators [Berner, 1989].

Although most existing simulators can estimate system performance such as bit error rate as a function of a particular coding and modulation scheme, they are incapable of predicting effects of the distance to and density of the scatterers, the channel bandwidth, or the vehicle antenna pattern. An exception to this is a simulation by Amoroso and Jones [1988], in which a random distribution of 1000 scatterers was assumed to exist in the plane of the vehicle's path. However, the drawbacks of this

study were its two-dimensional approach, which eliminated realistic elevation angle and antenna effects, and the avoidance of any scatterers in proximity to the vehicle, which in field measurements have been shown to dominate the signal variations in the absence of shadowing. The simulator described here remedies these deficiencies. It is an extension of a single scatterer multipath drive simulator [Vogel and Hong, 1988], which was based on simple physical and geometric considerations. The new version allows a vehicle to be driven through a region with many randomly distributed, point-source multipath scatterers. The output of the drive simulator are time series of signal amplitude and phase as well as Doppler spectra, all for user-specified conditions. These outputs, in turn, can be used to calculate system performance parameters. The simulator does not consider shadowing, and this limits its application to low fade margin systems, where multipath fading effects determine system performance most of the time. This is because shadowing tends to completely disrupt transmissions.

2. Model Derivation

The derivations are based on the single scatterer geometry shown in Figure 1, consisting of a satellite transmitting with wavelength w from given azimuth and elevation directions (θ_t,ϕ_t) relative to a vehicle moving with speed v along the x-axis, an arbitrary vehicle antenna pattern (directivity $D(\theta,\phi)$) , and a point-source scatterer s with a given scattering cross section σ and an arbitrary location. The resultant electrical field strength at the receiver is proportional to [Vogel and Hong, 1988]:

$$E_r(t) \propto 1 + \frac{\sqrt{\sigma}\cdot D(\theta_s,\phi_s)}{2\sqrt{\pi}R(t)D(\theta_t,\phi_t)} * \exp[-j\frac{2\pi}{w}[p-a(t)+R(t)]] \qquad (1)$$

where p-a(t) is the distance between the plane wave through the origin and the scatterer and R(t) is the distance between the scatterer and the vehicle antenna. The variable part of the sum is the contribution of the single scatterer. In order to obtain the total field at the receiver due to many scatterers, the vector sum of the constant incident field and all the scattered fields e is formed and the relative total power and phase are calculated from:

$$Power_{tot} = [(1 + \Sigma e_{real})^2 + (\Sigma e_{imag})^2]^{1/2} \qquad (2)$$

$$Phase_{tot} = \arctan[\frac{\Sigma e_{imag}}{1 + \Sigma e_{real}}] \qquad (3)$$

where the summation includes the real or imaginary parts of each scatterer's response e to the incident wave.

The power spectral density of the received wave is calculated by accumulating values of instantaneous power and Doppler frequency at 1000 samples per second, where the instantaneous frequency is the time derivative of the phase of the combined scattered waves, excluding the direct wave:

$$f_d = \frac{\delta(\text{Phase}_{scat})}{\delta t} = \frac{\delta}{\delta t} \arctan\left[\frac{\Sigma e_{imag}}{\Sigma e_{real}}\right] \quad (4)$$

All calculations were performed for time durations of 1 second, corresponding to a driving distance of about 25 m at a speed of 55 mph.

3. Model Validation

The operation of the model was validated by comparing the predicted power and phase assuming a single scatterer to the results from measurements, both with similar parameters. One example of this is shown in Figure 2, which depicts the situation in which the satellite illuminates the vehicle from 7 o'clock with an elevation angle of 35° at a frequency of 1547 MHz. The speed is 54 mph, and a scatterer (σ = 32 m²) is located 3 m to the right and 4 m above the vehicle antenna. The measured and calculated power time series are quite similar. Furthermore, parameters such as the position of the satellite or the scatterer were varied systematically, and the results changed consistently with expectations and measurements, where available.

Another test consisted of comparing the simulated power spectral density to the theoretically expected one [Clarke, 1968]. Figure 3 demonstrates that the simulation model produces the correct Doppler spectrum, centered on the received carrier frequency. The shape shows the typical signature of mobile propagation, a sharply bandlimited spectrum with maximum power at the edges. The frequency deviation of the scattered wave (±120 Hz) agrees with the value expected from the geometry.

4. Results

4.1 Comparison with 2D simulation

The two-dimensional simulation by Amoroso and Jones considered 1000 scatterers randomly distributed in an annular region with an outer radius of 2000 m and an inner radius of 400 m, corresponding to an average scatterer density of 12,000 m²/scatterer. Their simulated fading record of unmodulated carrier power for an omni-directional antenna, reproduced in Figure 4, shows peak-to-peak variations of over 20 dB. The corresponding output of the 3D simulator, for a drooping dipole antenna and with the height of the scatterers randomly distributed between 0 and 10 m, is shown in Figure 5. The range of the received power is less than 1.5 dB and this is in

agreement with measurements made in locations where no scatterers are in the vicinity of the vehicle.

4.2 Dependence of signal variations on clearance

Similar cases to the one above, except for an outer radius of 500 m and the much higher average scatterer density of 625 m^2/scatterer, were run with inner clearance radii from 30 to 400 m. The result, depicted in Figure 6, demonstrates that multipath phenomena for LMSS are significant only if the scatterers are located closely to the vehicle. The standard deviation of the logarithmic amplitude decreases monotonically with increasing inner clearance, from 0.22 dB to 0.07 dB.

4.3 Antenna pattern effects

In order to demonstrate the efficiency of high-gain antennas in reducing multipath interference, several calculations were performed with an antenna having 80° half power beamwidth in both azimuth and elevation planes. Tests with a single scatterer located either in the direction to the satellite or opposite to it resulted for the drooping dipole antenna in fades >10 dB (both cases) and for the high-gain antenna in fades >10 dB and <1 dB, respectively. The suppression of the multipath interference by the antenna patterns remains in effect as long as the antenna is pointed at the satellite.

In an environment with many scatterers, the reduction of the fluctuations is not as extreme, but still significant. For the case of 500 scatterers within a 10 to 300 m annulus, the peak-to-peak fluctuations were reduced by a factor of 4.5, from 7.2 dB to 1.6 dB.

5. Conclusion

A three-dimensional drive simulator has been used to calculate signal level time series for LMSS. The simulator allows the realistic inclusion of many scatterers in random positions as well as arbitrary antenna patterns. The major conclusions reached from this work are:

(1) Two-dimensional simulations overestimate multipath, because the elevation angle selectivity of the receiving antenna has to be neglected. Therefore they cannot be used to predict either amplitude, phase, or bandwidth effects realistically. (2) The three-dimensional simulator demonstrates that only scatterers in the immediate vicinity of the receiver matter. As a consequence, the delay spread spectrum is narrow and has no detrimental impact on contemplated systems with channel bandwidths of 5 kHz. (3) Time-series produced with this simulator will give more realistic inputs to systems which analyze bit error performance than those based on statistical assumptions only.

References

Amoroso, F. and W. W. Jones, " Modeling direct sequence pseudonoise (DSPN) signaling with directional antennas in the dense scatterer mobile environment", Proceedings of the 38th IEEE Vehicular Technology Conference, Philadelphia, PA, June 1988

Barts, R. M., W. L. Stutzman, W. T. Smith, R. S. Schmier, and C. W. Bostian, "Land mobile satellite propagation modeling", Proceedings of 1987 IEEE Antennas and Propagation Society International Symposium, Blacksburg, VA, June 1987

Berner, J. B., "Channel Simulator Upgrade to Use Field Propagation Data", contained in these proceedings

Clarke, R. H., "A statistical theory of mobile-radio reception", BSTJ, Vol. 47, No. 6, pp.957-1000, July-August 1968

Davarian, F., "Channel Simulation to Facilitate Mobile-Satellite Communications Research", IEEE Transactions on Communications, Vol. 35, No. 1, pp. 47-56, January 1987

Divsalar, D., "JPL's Mobile Communication Channel Software Simulator", Proceedings of the Propagation Workshop in Support of MSAT-X, January 30-31, 1985, JPL Internal Document D-2208, January 1985

Vogel, W. J. and U. S. Hong, "Measurement and Modeling of Land Mobile Satellite Propagation at UHF and L-Band", IEEE Transactions on Antennas and Propagation, Vol. 36, No. 5, pp. 707 719, May 1988

Vogel, W. J., J. Goldhirsh, and Y. Hase, "The Australian Experiment with ETS-V", contained in these proceedings

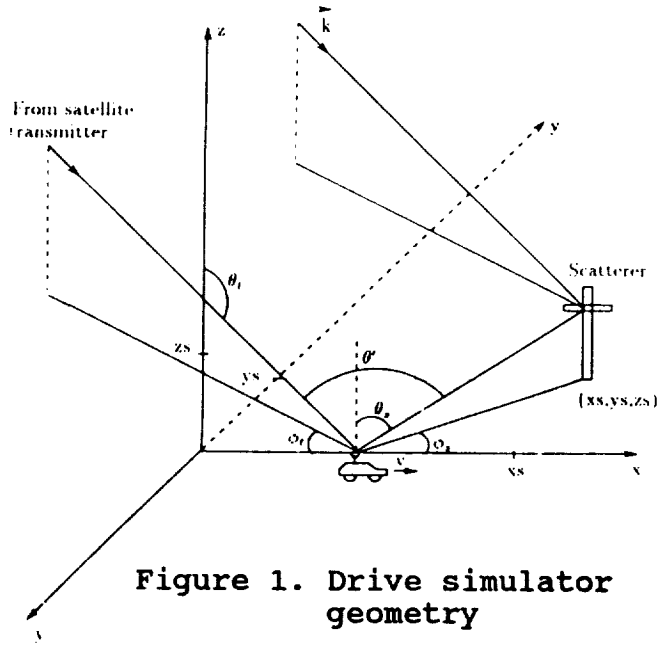

Figure 1. Drive simulator geometry

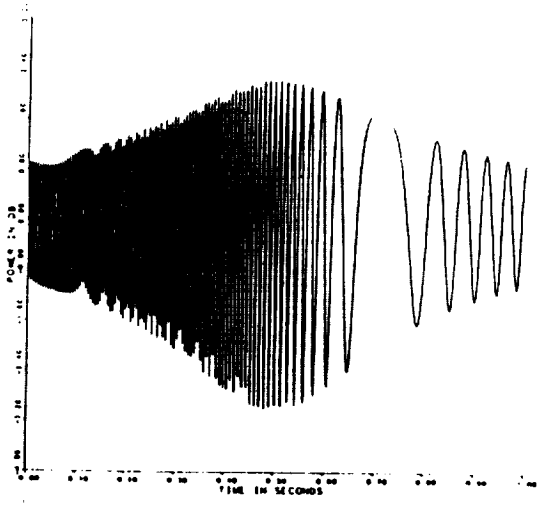

Figure 2. A single scatterer simulation output

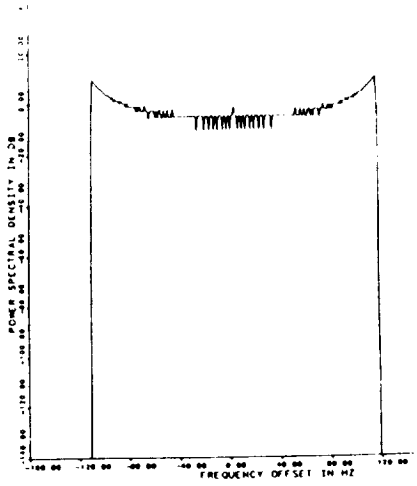

Figure 3. Doppler spectrum for one scatterer

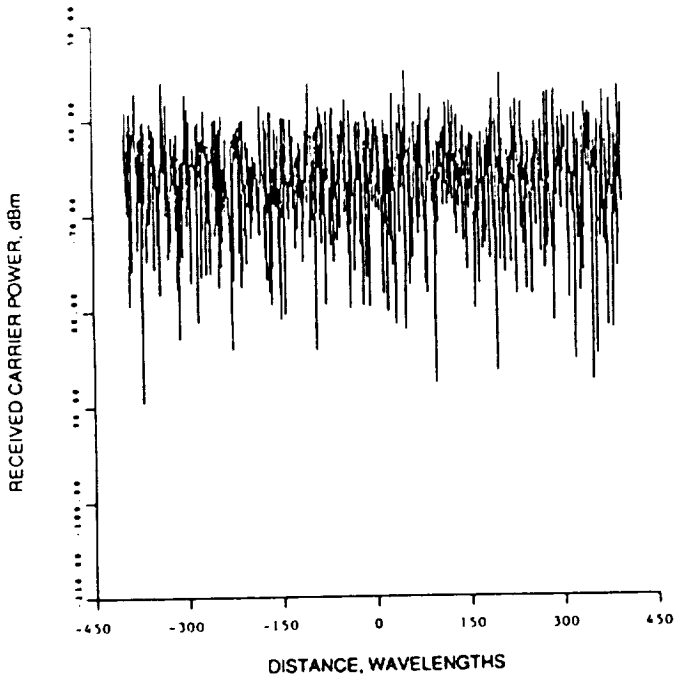

Figure 4. Amoroso's simulated fading record

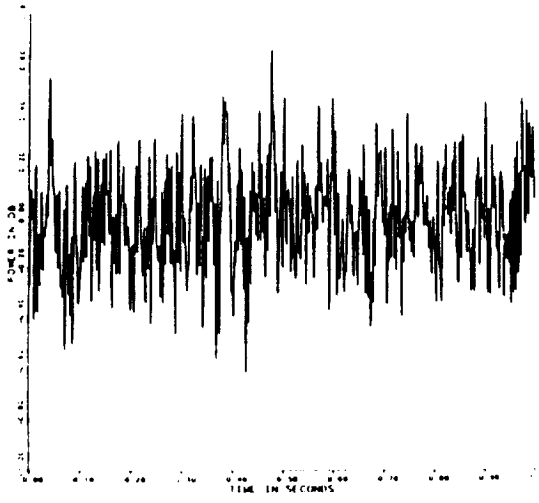

Figure 5. 3D simulation of 1000 scatterers

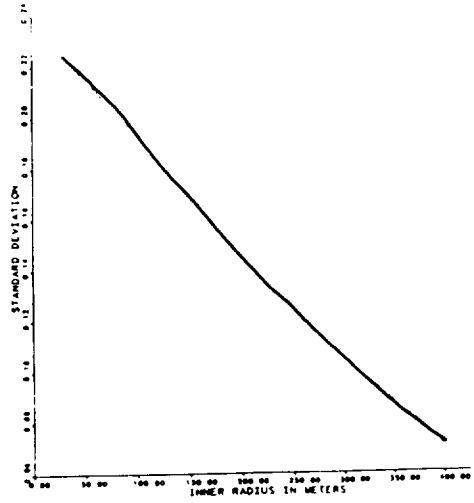

Figure 6. Power STDV as a function of inner clearance radius